



CERN-ACC-2015-0084

jean-christophe.gayde@cern.ch

HIE Isolde – General Presentation of MATHILDE

G. Kautzmann, J-C. Gayde, F. Klumb, Y. Kadi, CERN, Geneva, Switzerland
J. Bensinger, K. Hashemi, Brandeis University, Waltham, USA
M. Šulc, Technical University of Liberec, Liberec, Czech Republic

Keywords: HIE-ISOLDE, Survey and alignment, IWAA2014, Monitoring and Alignment Tracking for Hie-IsolDE, MATHILDE, Monitoring and Alignment Tracking for Hie-Isolde Software, MATHIS, HBCAM, Glass ball retroreflector.

Abstract

In the frame of the HIE-ISOLDE project a superconducting Linac will upgrade the energy and intensity of the REX ISOLDE facility at CERN. It will be made of 2 low- β and 4 high- β cryomodule. Each high- β cryomodule houses five superconducting RF cavities and one superconducting solenoid (respectively 6 and 2 for the low- β). Beam-physics simulations show that the optimum linac working conditions are obtained with components aligned and monitored on the Nominal Beam Line within 0.3 mm for the cavities and 0.15 mm for the solenoids at one sigma level. The Monitoring and Alignment Tracking for HIE-ISOLDE (MATHILDE) system is based on opto-electronic sensors, optical and mechanical elements partly exposed to high vacuum and cryogenic temperatures. This paper summarizes the MATHILDE studies and focuses on the viewport crossing, the MATHIS software, the newly designed HBCAM cameras and the retro-reflective targets based on high index glass properties.

Presented at: International Workshop on Accelerator Alignment, IWAA2014, 13-17 October 2014, IHEP, Beijing, P.R. China

Geneva, Switzerland
July, 2015

CERN-ACC-2015-0084
04/08/2015



HIE ISOLDE – GENERAL PRESENTATION OF MATHILDE

G. Kautzmann, J-C. Gayde, F. Klumb, Y. Kadi, CERN, Geneva, Switzerland
J. Bensinger, K. Hashemi, Brandeis University, Waltham, USA
M. Šulc, Technical University of Liberec, Liberec, Czech Republic

Abstract

In the frame of the HIE-ISOLDE project, most of the existing ISOLDE REX line will be replaced by a superconducting linac in order to upgrade the energy and intensity of the REX ISOLDE facility at CERN. This upgrade involves the design, construction, installation and commissioning of 2 low- β and 4 high- β cryomodules. Each high- β cryomodule houses five high- β superconducting cavities (6 for the low- β version) and one superconducting solenoid (2 for the low- β version).

Beam-physics simulations show that the optimum linac working conditions are obtained when the main axes of the active components, located inside the cryostats, are aligned and permanently monitored on the REX Nominal Beam Line (NBL) within a precision of 0.3 mm for the cavities and 0.15 mm for the solenoids at one sigma level along directions perpendicular to the beam axis.

The Monitoring and Alignment Tracking for Hie-IsoLDE (MATHILDE) system is based on opto-electronic sensors, precise optical elements, metrological tables and mechanical elements. Some of them will be exposed to non-standard environmental conditions such as high vacuum and cryogenic temperatures.

This paper summarizes the studies done for MATHILDE with special focuses on the viewport crossing, the software, the newly designed cameras (HBCAM) and the retro-reflective targets based on high index glass properties.

INTRODUCTION

The HIE-ISOLDE project is an upgrade of the ISOLDE REX facility and involves the design, construction, installation and commissioning of 2 low- β and 4 high- β cryomodules. The linac installation is staged in 3 phases. 2 high- β cryomodules will be installed during 2015, joined by 2 more in a second phase and 2 low- β cryomodules are planned to be added in a third stage.

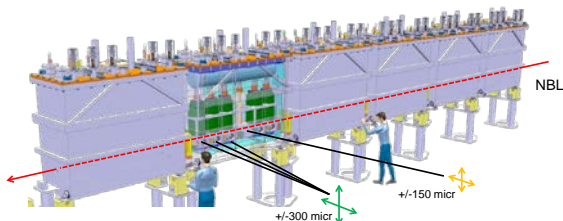


Figure 1: The HIE-ISOLDE linac

Each high- β cryomodule houses five high- β superconducting cavities (6 for the low- β version) and one superconducting solenoid (2 for the low- β version). To run the linac in the optimum conditions, the active components, cavities and solenoid, must be aligned and monitored on the REX Nominal Beam Line (NBL) within

a precision of 0.3 and 0.15 mm respectively at one sigma level along directions perpendicular to the beam [1].

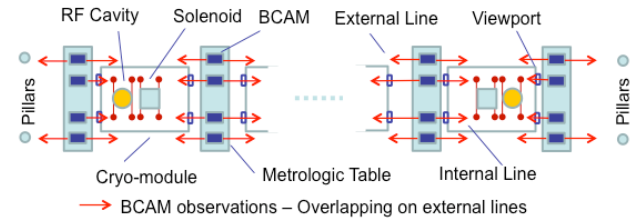


Figure 2: Sketch of the alignment system - Top view.

As sketched in Figure 2, the proposed alignment and monitoring system uses a set of newly developed double-sided HIE-ISOLDE Brandeis CCD Angle Monitor (HBCAM) [2] fixed to metrological tables in order to create a close geometrical network linked to the Nominal Beam Line by reference pillars. Two external lines of sight, one on each side of the cryomodule, are created and act like a frame. The HBCAM from the internal lines are placed in front of viewports and allows the observation of targets attached to the active elements and of the HBCAMs situated on the previous and next table.

The project requires the study of the optical effect of measurements through precise viewports [3], the creation of a dedicated 3D-Reconstruction Software [4], of precise mechanical parts [3], an upgrade of the foreseen BCAM devices and the development of a new type of targets based on high index glass ball properties.

THE HBCAMS

In the high- β cryomodule, 6 active elements are to be monitored. Each active element have 4 targets attached, creating two lines of targets placed in front of the viewports (as shown in Figure 2 and 3).

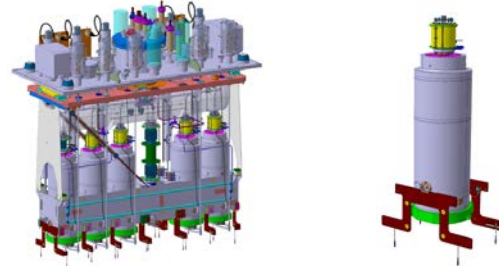


Figure 3: View of an opened cryomodule (left), One cavity on its supporting plates and monitoring targets hanging on the bottom (right)

Therefore, each line has 12 targets to measure placed in a special spatial distribution in order that they do not shadow each other. The field of view of the original BCAM is too tight to maximize the number of target seen by one

device (see Figure 4); therefore a new evolution of the BCAM, called HBCAM has been developed in collaboration with Brandeis University.

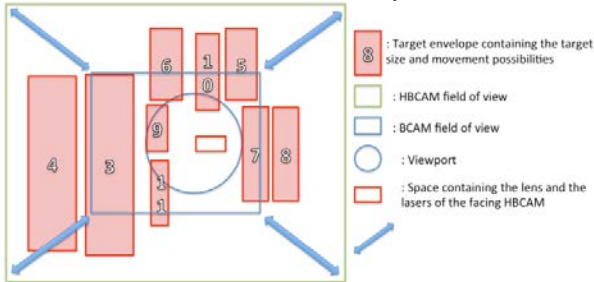


Figure 4: View of what a device will see inside the high-β cryomodule: 9 targets (out of 12).

The HBCAM is a metrology device with two cameras facing in opposite directions, two pairs of laser diode light sources, and four white LED flash arrays. The cameras, lasers, and flash arrays are assembled in one anodized aluminum chassis that sits on a three-ball kinematic mount. In a metrology system, the HBCAMs are arranged so that they can view one another's sources. They may also view sources that have no cameras associated with them, such as flashing optical fibers, retroreflectors, and internally lit ceramic spheres. In the HIE-ISOLDE application, the HBCAMs will flash each other and some of them will also observe the image of their own lasers in retroreflecting glass spheres.

The HBCAM is the first BCAM to use the ICX424AL monochrome CCD image sensor from Sony Semiconductor. The sensor's image area is 5.2 mm x 3.8 mm. The long side of the image sensor is parallel to the plane containing the kinematic mounting balls, and the short side is perpendicular to this plane. The LWDAQ system can read out the image either as 520 x 700 pixels each 7.4 μm square, or as 260 x 350 pixels each 14.8 μm square. The 7.4 μm pixel readout provides better measurement precision for sharply-focused spots. The 14.8 μm pixel readout provides 3 image/s readout rate with the LWDAQ Driver (A2071E).

Each HBCAM camera has a single 6 mm diameter, 48 mm focal length plano-convex lens to form its images. The distance from the lens to the image sensor is roughly 50 mm, with the sharpest focus at range 1.5 m. The field of view of the camera is 100 mrad in the plane of the mounting balls and 75 mrad perpendicular to this plane. This is more than double the field of view of the BCAMs installed in the ATLAS detector.

The HBCAM lasers are 7 mW 650 nm laser diodes in metal cans. The cans are mounted in holes on either side of the camera lenses, so that each lens has a pair of lasers to view in a retroreflector, or to view from another HBCAM. To obtain consistent output power from the HBCAM lasers, each laser is calibrated during construction. The resistor value is adapted to set the output power to 5 mW. As a result, the output power of the HBCAM lasers lies in the range 4.5-5.5 mW. The consistent output power of the HBCAM lasers gives a way to identify image acquisition problems by estimating how bright the lasers should appear

in the images. Moreover it offers standardization in the measurement parameters for retroreflective targets.

The HBCAM is the first BCAM to provide an array of LEDs to generate a flash of light that can be seen in targets of retroreflecting tape. The flash is bright enough that retroreflecting tape targets several meters away can be identified and located with standard BCAM analysis.

The HBCAM measurement precision is expected to be 5 μrad across the entire field of view, this being the precision obtained with ATLAS BCAMs. Indeed, the HBCAM image pixels each subtend 150 μrad at the center of the camera aperture, which is similar to 130 μrad subtended by the pixels of the ATLAS BCAMs. The precision of the ATLAS BCAMs was limited by atmospheric turbulences at long range (> few meters) and by image sensor irregularities at short range (<1m). Compared to the ATLAS BCAMs, no image sensor irregularities were observed so far with the new CCD.

The Figure 5 shows how the separation of two laser images changes as we move the two lasers across the field of view of an HBCAM. The camera is focused at range 1.5 m and the pair of red lasers is at range 2.5 m. The obtained precision is at 4 μrad level which is consistent with the expected 5 μrad.

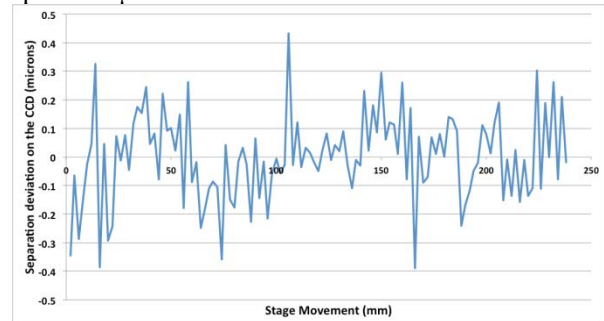


Figure 5: Image Separation Deviation

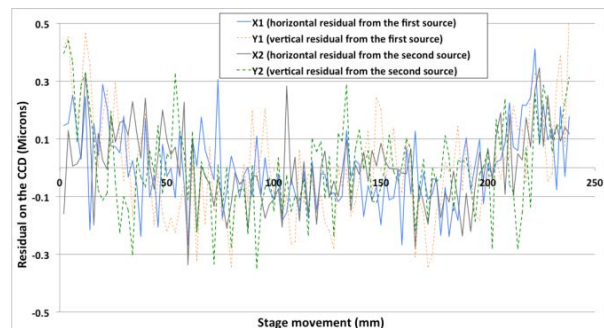


Figure 6: Non-Linearity Across Entire Field of View. Residuals in microns on the image sensor, plotted against stage position.

In the same conditions, the Figure 6 shows the residuals from a straight line fit to the position of two lasers moving across the field of view. The achieved precision is about 4 μrad for the lateral movement.

The absolute accuracy of the HBCAM is dominated by the quality of the calibration. The same roll-cage arrangement than for the ATLAS BCAM is used to calibrate the HBCAM. The ATLAS BCAM calibration

accuracy was 50 μrad in source bearing, 20 μm in pivot point position, and 20 μm in source position.

The HBCAM calibration of pivot point and source position is consistent with the ones observed for the ATLAS BCAMs. Within the field of view of an ATLAS BCAM, which is roughly ± 25 mrad from the nominal camera axis, the HBCAM calibration is expected to be at a level of 50 μrad , as for the ATLAS BCAMs.

Outside of the ± 25 mrad, extending to the ± 50 mrad field of view of the HBCAM, it is possible for the existing calibration to not provide 50 μrad absolute accuracy. The HBCAM could suffer from optical aberrations that were negligible for a smaller field of view camera. Some sign of those effects were observed but staying below a 5 μrad precision level. Therefore the calibration of the center of field of view should apply to the outer edges of its field of view, but if bigger effects are observed on some devices, additional parameters -derived from a photogrammetric approach - will be calibrated.

The HBCAMs and associated electronics for a 6 cryomodule configuration are procured. The procurement includes 56 HBCAMs, 4 Drivers and 14 Multiplexers, enough to cover a 6 cryomodule configuration linac, follow up during assembly/cryo-tests and unexpected device failures or damages.

THE TARGETS

Introduction and target support

The targets are attached to the supporting plates of the active element [3] and therefore are subject to high vacuum and cryogenic conditions at 4.5 K. The main constraints for them are: to be vacuum compatible; to work at 4.5K; to be measurable from several directions and to have a narrow shape (6mm max) to stay in their allocated envelope. The targets presented in [3] have drawbacks that led to the development of a new solution based on the optical properties of the high index glass ball lenses. Those lenses are made from S-LAH79 material, produced by OHARA Inc. [5], which offers a refracting index of about 1.993 for the HBCAM laser wavelength (650nm).



Figure 7: Pictures of the final target design. Top on the left, bottom on the right

Figure 7 shows the final design of the target. The titanium made body is 6mm diameter. The spring, the 4mm diameter glass and ceramic balls are loaded from the bottom. Once those elements are inserted, the target is close by a plug hold in place by a 2mm diameter pin. The design allows housing several glass balls in one support. As sketched in Figure 7, a configuration with 2 glass balls spaced by 2 precise ceramic balls is foreseen as the standard target inside the cryomodule. To increase the redundancy of the system, the targets allow multidirectional observations: most of the glass balls can

be observed from the 2 HBCAMs, placed upstream and downstream of one cryomodule on the same internal line. The target comes into 5 different lengths between the middle pin and the last glass balls in order to maximize the number of targets measurable (see Figure 4). The targets are guided by a V groove into the supporting plate of the active elements, blocked in height by a pin and fixed by a screw. The target has been designed in order to be vacuum compatible. The tested outgassing rate for an amount of glass spheres sufficient to equip one full high- β cryomodule stays at the sensitivity limit of the used outgassing system (below $3.8 \cdot 10^{-8}$ mbar*L/s) and therefore is negligible compared to the total gas load budget of $2 \cdot 10^{-4}$ mbar*L/s of a cryomodule. Cryogenic tests have been performed using a HBCAM observing glass ball targets sitting in a cryostat through an inclined viewport. Neither specific behavior nor damage was observed down to 5K and $40 \cdot 10^{-6}$ mbar.

High Index Glass balls theory

Glass ball, made from high refractive index glass, can partially reflect light backwards to the light source. Beam, falling into the sphere surface at angle α , is refracted to angle β , obeying the Snell law. It is deflected with $\alpha - \beta$ at point A. Part of the beam is reflected on the opposite side at point B and going out from the sphere with the change of direction $\pi - 2\beta$. Beam is refracted again at the output C from ball by the angle $\alpha - \beta$. The emerging beam direction forms an angle $\pi + \gamma$ with the direction of original beam, as it is shown on Figure 8. If we define the oriented angle γ to be positive for diverging input and emerging beams (for small refractive index), and negative for crossing beams (high refractive index) as is shown on Figure 8, the final deflection angle can be described by the equation

$$\gamma = 4\beta - 2\alpha$$

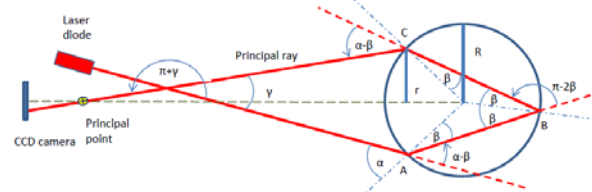


Figure 8: Schematic drawing of the beam path in a glass ball with a refractive index of 2.0

A simple model can be assumed: the ball is far from the laser diode (radius R is many times smaller than this distance), and is illuminated by an almost parallel beam. The principal ray, passing by the camera principal point with the direction γ , seems to come from point C. This point is at a distance r from the optical axis connecting the center of the ball to the camera principal point. This simple equation is therefore valid:

$$\sin\alpha = r/R$$

If Snell's law is taken into account, γ can be expressed for a ball with a refractive index n by:

$$\gamma = 4 \cdot \arcsin\left(\frac{1}{n} \frac{r}{R}\right) - 2 \cdot \arcsin\left(\frac{r}{R}\right)$$

The solution of this equation is drawn in the Figure 9 for different refractive indexes.

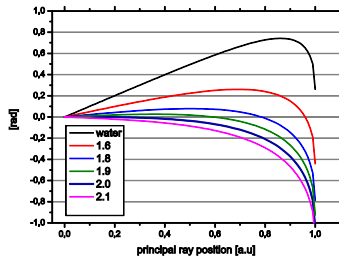


Figure 9: Deflection of the beam, depending on relative principal ray position, given by r/R ratio

This figure can explain both rainbow (water drop, $n = 1.33$, most of the light is deflected about 0.75 rad) and exceptional properties of balls with refractive index equal to 2.0. Almost all beams, falling to the ball are reflected to the light source (deflection is below 1 mrad for $r/R < 0.16$, and 10 mrad for $r/R < 0.34$).

A more sophisticated model was made, but it doesn't differ from the simple one for more than 1%. Also it is not necessary to take into account the external reflection on the first surface or the effects of the two inner reflections, because their reflections toward the camera is almost negligible in both cases.

The inverse problem for targets must be solved. The angle γ is fixed by geometry - ratio of distance between the laser diode and the camera principal point over the distance to the ball. The beam spot observed in the imaging system is not in the center of the ball. This effect is due to the offset between the observing point and the flashing laser source. The observed relative position r/R of the spot inside ball image is described by the previous equation. The observed spot intensity profile is asymmetrical due to the spherical aberration on the ball surface. For two laser diodes, symmetrically placed on the both sides of HBCAM lens, two spots on the ball surface are observable with a symmetrical intensity profile. The left spot correspond to left source, and vice versa. The centers of gravity of these two spot images correspond to the center of the ball image. The distance between the spots is function of the angle γ only, so the variation of this distance due to lateral ball movement within the HBCAM field of view boundaries is negligible.

Test Results

The theoretical relation between the incidence angle and the radius ratio presented in Figure 9 has been tested by HBCAM observations on a 10 mm diameter high index glass ball. The Figure 10 shows that the measured points are matching the theoretical curve. The error observed between the reference curve and the measured points is at a range of 4%. This effect is explained by the asymmetrical intensity profile of the spots. But as both flashes on the HBCAM, symmetrically placed around the pivot point, are

used to determine the center of the glass sphere, the asymmetrical effect is cancelling itself.

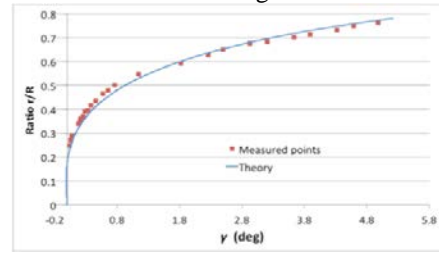


Figure 10: Ratio r/R plotted against γ .

The precision of the reconstruction of a lateral movement (with respect to the HBCAM optical axis) has been tested by taking measurements on two 4mm diameter high index glass balls encapsulated in one of the target prototypes. The movement is done by a micrometer stand and controlled by an AT401 Laser Tracker. The average offset observed between the HBCAM reconstructed movement and the one from the Laser Tracker is within a few microns with a precision at one sigma level of 10 μm (Figure 11) in object space. This test has been done for a lateral translation of 47mm at a distance of 1.2m, covering approximately 40% of the field of view starting from one of its edge. Those values are consistent with other tests performed.

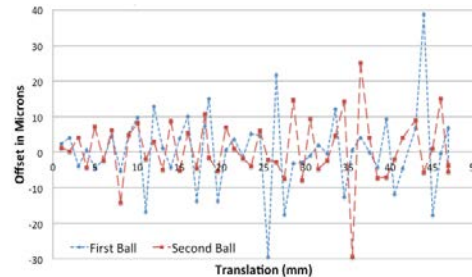


Figure 11: Graph of the offset in object space between a nominal movement and the one reconstructed by HBCAM measurements. The figure displays two sets of measurements done with two different glass balls.

THE VIEWPORTS

Most of the studies are presented in the reference [3]; their outcomes for a 6.55mm thick fused silica viewport mounted in a CF63 flange were that:

- The wedge angle needs to be limited to 10 arc/second for MATHILDE;
- The parallel plate effect is tested and validated, for small angles, 1 degree rotation of the viewport with respect to the nominal line of sight induces a radial displacement of the target of about 35 μm ;
- The glass deformation due to vacuum pumping is negligible.

With the use of targets based on high index glass balls, a flashing HBCAM observes the mirror image of its own light spots in the targets. The flash time needs to be increased (compared to active target measurements) and therefore creates perturbation in the measurements through the viewport. If the viewport face is perpendicular to the

HBCAM Principal Vector, i.e. the vector coming from the center of the CCD to the pivot point of the HBCAM, parasitic reflexions occur and make the measurement impossible. To resolve this issue, two solutions were considered:

- Anti-reflection surface coating for the wavelength range of the HBCAM Laser (650nm).
- Tilting the viewport to direct the reflections out of the HBCAM Field of view.

To keep the same glass material, validated geometrically, optically and for his behaviour in cold and vacuum conditions, the second option was studied and tested. The outcome is that the viewport shall be tilted by 2 deg. around X axis or 3 deg. around Y axis (Figure 12). Therefore, the supporting system of the viewports on the cryomodule can be either: adjustable or designed to include this angle into the CF63 mounting flange.

Due to integration issues in the inter-cryomodule region, the second solution was adopted and viewports are mounted into the CF63 flange with a 5 degree angle (with respect to the external surface of the flange).

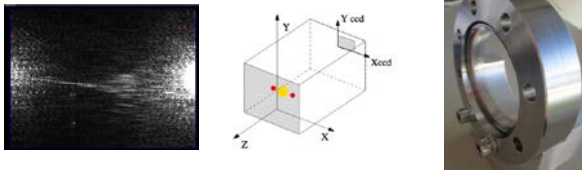


Figure 12: HBCAM image showing the parasitic reflection in the glass (left), Definition of the axis [3] (center), Picture of a tilted window in its flange (right)

The final product has been developed on purpose in collaboration with CERN's vacuum experts and industry. The procurement for the 2 first cryomodules is completed. The validation tests have been successfully performed in order to, amongst other, verify the inclination of the viewport in its flange (5 ± 0.5 degrees) and the glass wedge angle (< 10 arc/second). For this last point, a specific method of verification has been established: the tilted glass introducing complexity into the measurement by standard methods.

THE METROLOGICAL TABLES

At the end of the linac and between each cryomodules, a metrological table housing 4 HBCAMs is inserted. The table is passing through metrology in order to have the geometrical relations between the 4x3 HBCAM supporting balls and, also, the link to the fiducial marks. The critical values are the relative orientations between each device; a special adapter reproducing the HBCAM supporting interface will be designed to improve the relative angle observations.

The adjustable metrological tables are close to a final design. The pieces seen in Figure 13 will be inserted as an ensemble in the intertank region in order to keep the calibration measurements. This ensemble includes two sub-assemblies: the supporting plates and the actual metrological table.

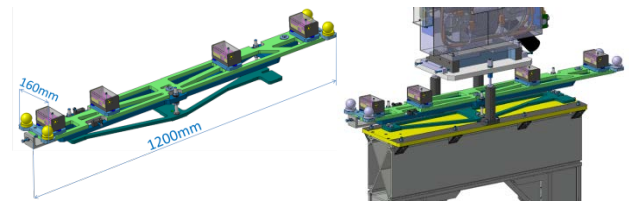


Figure 13: Picture of a metrological table prototype (light green) on its adjustable support (dark green) (left), integrated in its inter-cryomodule region (right)

The first sub assembly comprises a base plate equipped with 3 threaded rods on top of which a second plate can be levelled. The metrological table includes:

- A base table sliding and adjustable on the top supporting plate.
- 4 interfaces housing the HBCAM mounting balls fixed on the base table. These outer pieces are elevated with 3 rods on some table in order to stage the HBCAMs in height to create overlapping measurement [3].

The pieces are pierced with opening in order to decrease their own weight whilst keeping most of their rigidity. The full ensemble weight only around 11kg.

This set-up has been optimised to attenuate as much as possible the impact of vibrations potentially introduced by the vacuum turbo pumps of the Diagnostic Boxes sitting in the vicinity.

THERMAL SHIELD CROSSING

As shown in Figure 14, thermalized corridors have been introduced in the design of the thermal shielding. They allow the targets to cross them with a minimal addition to the heat load of the cavities and solenoids whilst keeping them visible from the HBCAMs. Non reflective aluminum plates cover the inner part of the corridor to minimize potential parasitic reflection on the HBCAM images.

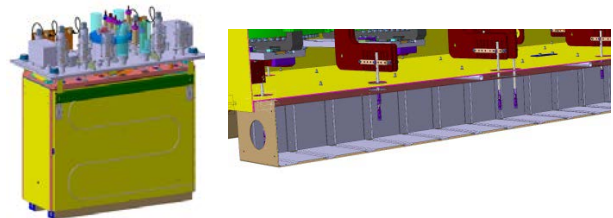


Figure 14: Thermal shield the two alignment corridors on the bottom (left), cut away detail view (right).

THE MATHIS SOFTWARE

The general Monitoring and Alignment Tracking for Hie-Isolde -Software (MATHIS) philosophy and concept validation is presented in [4] and is inspired by ARAMyS software [6]. To sum up, every element, even a point, has a coordinate system attached to it. All the frames are placed in a hierarchical order where one frame can only have one parent but several child systems. The geometrical link between frames is described by 6 transformation parameters (3 translations, 3 rotations), each of them can be constraint or not and can be parameterized by a formula

depending on temperature and pressure in order to cope with the thermal expansion of the mechanical pieces. Each frame can have some options depending on their type (active/passive targets, viewport, etc...) allocated to them. For instance, the additional options for a glass ball target are its refractive index and diameter. The goal is to recalculate each free parameter by a 3-D adjustment taken into account the HBCAMs measurement done between themselves, on targets and on reference points. This highly versatile and flexible principle allows virtually to create any kind of system configuration using BCAM or HBCAM.

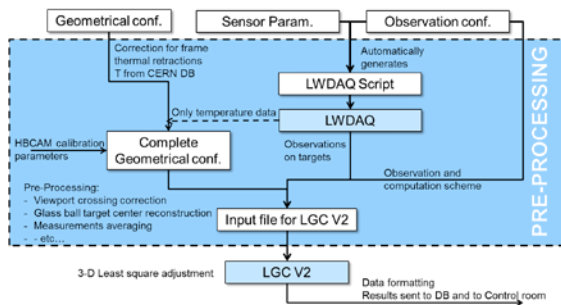


Figure 15: MATHIS data flow

On a practical point of view, a whole system is described by 3 XML files. The geometrical file declaring all the coordinate frames and describing all their links and associated parameters. The sensor one defining each type of sensor allowed into MATHIS. The observation configuration file declares: which device is installed on which coordinate frame; how to address each sensor; which targets is measured by which device and what is the chosen computation scheme.

Those 3 files are going through a pre-processing routine. By retrieving the temperature of some mechanical piece inside and outside the cryomodule, the geometrical configuration file is corrected for the thermal expansion with the formulas expressed in this same file. Indeed, a change of temperature acts on the transition between frames. This step also includes the automated creation of several frames related to the HBCAM calibration file. Indeed each component (pivot point, laser sources, etc...) of an HBCAM is transformed in a coordinate frame.

By combining the sensor and geometrical observation files, MATHIS creates automatically an LWDAQ script making the observations. LWDAQ is the software managing the HBCAM measurement, as well as, all the Open Source Instrument devices [2].

With the observations, the corrected geometrical configuration and the observation configuration file, MATHIS is able to calculate the viewport crossing effect and to compute the corrected observation at the high index glass ball centre. In the case of observations crossing two viewports, an equivalent viewport is determined [3]. Once this step is passed the pre-processing ends by creating entry data to be processed by the LGC V2 CERN 3D adjustment software.

LGC V2 is being updated in order to cope with a hierarchical set of frames and with laser tracker

observations. The BCAM type sensors are considered as laser trackers with distance measurements loosely weighted and determined from the a priori positions. One laser tracker like instrument is automatically created on each device pivot points and the CCD measurements are transformed in 2 angles. The LGC V2 result is formatted and sent to the Control room.

CONCLUSION

MATHILDE has proven its feasibility in [3, 4]. The new devices and mechanical parts are giving good results in accordance with the needed precision. Most of the parts are integrated and designed or close to a final one.

The HBCAM developed for the project are answering fully to the specifications and alignment needs. They are a major improvement of the oldest version and are already considered in other projects.

The newly developed multidirectional retroreflective imaging target based on high index glass balls give very good results with HBCAM measurement and are resilient to high vacuum and cryogenic conditions.

The software development is well advanced. LGC V2 will be integrated in the process. Tests to validate all the data flow and 3D-reconstruction are foreseen in the near future.

The goal is to be ready to install the first alignment system once the first cryomodule is toward the end of its assembly and ready for vacuum and cryogenic tests.

ACKNOWLEDGMENT

We would like to acknowledge the receipt of fellowships from the CATHI Marie Curie Initial Training Network: EU-FP7-PEOPLE-2010-ITN Project number 264330.

We acknowledge also funding from The CATE (Cluster for Accelerator TEchnology) Consortium EU regional program Interreg IV and from the Belgian Big Science program of the FWO (Research Foundation Flanders) and the Research Council K.U. Leuven.

REFERENCES

- [1] M.A.Fraser et al, Phys. Rev. ST Accel. Beams 14,020102 (2011).
- [2] BCAM, <http://alignment.hep.brandeis.edu>.
- [4] J-C. Gayde, G. Kautzmann et al, "HIE-ISOLDE Alignment and Monitoring System Technical Design and Project Status", IWAA2012, Chicago (2012).
- [3] J-C. Gayde, G. Kautzmann et al, "The HIE-ISOLDE Alignment and Monitoring System Software and Test Mock-up", IWAA2012, Chicago (2012).
- [5] OHARA Inc. <http://www.ohara-inc.co.jp>
- [6] C.Amelung, "ARAMyS – Alignment Reconstruction Software for the ATLAS Muon Spectrometer", 10th Topical Seminar on Innovative Particle and Radiation Detectors, Sienna (2006).